Journal of Electronic Imaging

JElectronicImaging.org

How much image noise can be added in cardiac x-ray imaging without loss in perceived image quality?

Amber J. Gislason-Lee
Asli Kumcu
Stephen M. Kengyelics
David S. Brettle
Laura A. Treadgold
Mohan Sivananthan
Andrew G. Davies

SPIE. IS&T imaging.org

How much image noise can be added in cardiac x-ray imaging without loss in perceived image quality?

Amber J. Gislason-Lee,[a,*] Asli Kumcu,[b] Stephen M. Kengyelics,[a] David S. Brettle,[c] Laura A. Treadgold,[a] Mohan Sivananthan,[d] and Andrew G. Davies[a]
[a]University of Leeds, Division of Biomedical Imaging, Worsley Building, Clarendon Way, Leeds LS2 9JT, United Kingdom
[b]Ghent University, iMinds-IPI, Sint-Pietersnieuwstraat 41, Ghent B-9000, Belgium
[c]Old Medical School, Radiological Physics, Leeds Teaching Hospitals Trust, Leeds LS1 3EX, United Kingdom
[d]Yorkshire Heart Centre, Leeds Teaching Hospitals Trust, Great George Street, Leeds LS1 3EX, United Kingdom

Abstract. Cardiologists use x-ray image sequences of the moving heart acquired in real-time to diagnose and treat cardiac patients. The amount of radiation used is proportional to image quality; however, exposure to radiation is damaging to patients and personnel. The amount by which radiation dose can be reduced without compromising patient care was determined. For five patient image sequences, increments of computer-generated quantum noise (white + colored) were added to the images, frame by frame using pixel-to-pixel addition, to simulate corresponding increments of dose reduction. The noise adding software was calibrated for settings used in cardiac procedures, and validated using standard objective and subjective image quality measurements. The degraded images were viewed next to corresponding original (not degraded) images in a two-alternative-forced-choice staircase psychophysics experiment. Seven cardiologists and five radiographers selected their preferred image based on visualization of the coronary arteries. The point of subjective equality, i.e., level of degradation where the observer could not perceive a difference between the original and degraded images, was calculated; for all patients the median was 33% ± 15% dose reduction. This demonstrates that a 33% ± 15% increase in image noise is feasible without being perceived, indicating potential for 33% ± 15% dose reduction without compromising patient care. [DOI: 10.1117/1.JEI.24.5.051006]

Keywords: angiography; cardiac x-ray imaging; image processing; simulated image noise; subjective image assessment; radiation dose.

Paper 15386SSP received May 15, 2015; accepted for publication Sep. 9, 2015; published online Oct. 27, 2015.

1 Introduction

Dynamic x-ray imaging systems are essential for diagnosis and treatment of coronary heart disease, which is the most common cause of death world-wide.[1] During percutaneous coronary interventional (PCI) procedures, real-time images of the moving heart allow visualization of anatomy and clinical devices inside the human body. In angiography, cardiologists use live, high-quality moving images of the coronary arteries for diagnosis. If there is a narrowing of an artery which restricts blood flow, the patient is treated via image-guided angioplasty; interventional devices such as guide wires, balloons, and stents are manipulated using lower quality x-ray imaging known as fluoroscopy. X-ray image quality must provide high enough spatial resolution to visualize a small arterial narrowing, and high enough temporal resolution to visualize blood flowing through the arteries; however, the image quality is directly related to the amount of radiation used to capture the image.

Exposure to x-rays is harmful, and radiation doses from interventional cardiac procedures are the highest of any routine medical procedure.[2] Patients have been reported to suffer from hair loss and transient and permanent skin damage caused by cardiac procedures;[3–6] these effects are known to occur when the radiation dose exceeds a specific threshold.[7] Multiple high-dose procedures being performed on relatively young patients may cause radiation-induced genetic effects and cancer later in life;[8] several decades may pass before these latent effects manifest. Risk of latent effects is cumulative, increasing with radiation exposure, however, there is no specific threshold dose.[7]

Clinical personnel are also at risk of these latent effects, due to their close proximity to x-ray scatter; there may be 6 to 12 staff members working in the x-ray room for a given cardiac procedure. Tumors have been reported in interventional cardiologists, dominantly on the same side of the body as would receive the most x-ray scatter.[9] Standard protective shielding does not provide staff with full head and body protection from prolonged exposure. Radiation dose from a single patient case poses little risk; however, over a working lifetime the cumulative radiation dose received by cardiologists can be high.[10] In addition, eye lens cataracts are common among interventional cardiologists;[11] cataracts are known to occur when the eye dose exceeds a specific threshold, and recently the international authorities reduced the threshold eye dose by 75%.[12]

In 2012, over 92,000 interventional cardiac procedures were performed at 118 centers in the UK; these figures have doubled since 2002,[13] illustrating the rise in the number of procedures and associated rising risk. As equipment continues to advance, longer, more complicated cases are undertaken. This coupled with the increasing age of the population suggests that the frequency of these procedures will continue

*Address all correspondence to: Amber J. Gislason-Lee, E-mail: a.j.gislason@leeds.ac.uk

to increase. It is, therefore, clear that efforts must be made to set the radiation dose as low as reasonably practicable (ALARP) without compromising patient care.

It has been suggested, specifically for cardiac x-ray imaging, that image quality is often higher than is required for the clinical task,[14] causing unnecessarily high levels of radiation dose to both patients and personnel. The aim of this research is to determine by how much the radiation dose can be reduced before image quality as perceived by clinical professionals, and hence patient care, is compromised. The lowest dose level achievable for the required level of image quality has not been investigated for cardiac x-ray imaging using clinical (patient) images, according to the literature. Two bespoke software programs—an image processing program to replicate patient images at multiple radiation dose levels, and an image assessment program to measure cardiologists' perceptions of these images—were developed to achieve the study aim. A small set of patients were used to determine the feasibility of further, larger scale work of this type.

2 Methods

2.1 *Noise Simulation Software SimDR*

To ascertain the optimal level of radiation dose for a patient image, that image must be assessed at various dose levels. It is unethical to repeatedly expose a patient to radiation to capture the same image with varying dose levels. Therefore, the software program *simDR* was developed in MATLAB® (The Mathworks Inc., Natick, Massachusetts) to simulate natural image degradation that would occur by reducing the dose on the cardiac x-ray system used in this study. Noise is directly related to radiation dose; for the given x-ray system the relationship between noise and radiation dose was extensively studied and quantified, allowing for the development of *simDR*. Images could then be degraded by adding noise to simulate a corresponding reduction in the radiation dose used to capture the images.

2.1.1 *Software calibration*

Given the x-ray system's proportionality between pixel intensity and input dose, since x-ray quantum noise is Poisson distributed, it follows that the variance is proportional to pixel intensity. This proportionality depends on x-ray beam energy,[15] therefore, a calibration model relating variance and pixel intensity was created for the range of beam energies pertinent to cardiac interventional x-ray imaging. The calibration model permitted calculation of the appropriate amount of noise to add for a given beam energy.

Calibration images were captured on an Allura Xper cardiac interventional x-ray system (Philips Healthcare, the Netherlands) in the cardiac catheter suite at Yorkshire Heart Centre, Leeds General Infirmary, UK, using the left coronary digital ("cine") acquisition mode at 15 frames/s (standard default angiography mode). The total filtration of the x-ray tube, not including additional prefiltration, was 2.5 mm aluminum (Al). The attenuation equivalent of the patient table was 1.43 mm Al, measured at 100 kV with a 3.7-mm Al half value layer. The manufacturer allowed for image data capture without the routine digital enhancement which is used on clinical images. The logarithmic look-up table which was used to transform pixel intensities as a preprocessing stage was provided by the manufacturer, and its inverse was applied to all images in order to restore the linear relationship between radiation dose and pixel intensity values. Images of 1024×1024 pixels were exported with an 8-bit depth in a Philips Healthcare proprietary format.

Flat field image sequences of polymethyl methacrylate (PMMA) blocks 20, 25, 30, and 35 cm thick were acquired with source to image detector distances (SID) of 97, 102, 107, and 112 cm, respectively, in the posterior anterior (PA) projection, with the C-arm rotated to place the x-ray tube near the floor. These PMMA thicknesses represent a realistic range of adult chest thicknesses, measured in the PA projection. The automatic dose rate control (ADRC) was used to determine the peak tube voltage, peak tube current, and x-ray pulse duration (hereafter called radiographic factors) which would be used in clinical practice for each thickness. For this x-ray system, the peak tube voltage is selected automatically based on an internally-calculated patient-equivalent thickness, which depends on the patient size, the anatomic projection angle, and the spectral beam filtration;[16] peak tube voltage was used to characterize x-ray beam energy.

For each beam energy, image sequences were captured for a range of dose levels using settings simulating clinical practice in acquisition mode. Radiographic factors were selected manually by overriding the x-ray system's ADRC; the range of dose levels (set by varying peak tube current and x-ray pulse duration) was as wide as practicable considering the x-ray system's intrinsic limits on radiographic factors (see Table 1). The antiscatter grid (13:1 grid ratio, 70 lines per cm, and 100-cm focal length) and spectral filtration (0.1 mm Cu + 1.0 mm Al) were in place. The patient table was 90 cm above the floor, with a 10-cm air gap between the exit surface of the phantom and an antiscatter grid for all images. This geometry was chosen to replicate patient image acquisition settings, and phantom image sequences were 3 s long.

Entrance surface dose rate (ESDr) to the phantom was the dose reference used to create and test the software, measured using a 20X6-6 ionization chamber and 2026C dosimeter (Radcal Corporation, Monrovia). The ionization chamber

Table 1 Radiographic factors used to calibrate noise simulation software.

Peak tube voltage (kVp)	Peak tube current (mA)	Pulse duration (ms)
69	100, 200, 300, 400, 500, 600	5
69	600	10
75	200, 400, 600, 800	6
75	800	12
92	300, 500, 700	8
92	700	12
118	300, 400, 500, 565	10

was placed between the phantom and the patient couch, using 5-cm thick wood spacers on the patient table.

Variance and mean pixel intensity were calculated for each image sequence. Prior to all variance calculations, spatial effects from the antiscatter grid and x-ray scatter were removed using linear frame subtraction (a valid method for static flat field images), to ensure only true variations of the mean were considered in the calculation. To account for the frame subtraction (which doubles the variance), variance was divided by two. For each beam energy, variance was plotted as a function of mean pixel intensity at all dose levels and a linear fit was calculated; the gradient and y-intercept of these linear fits were used as follows: the mean of the y-intercepts was calculated and this single offset value represented the noise in an unexposed image. The four gradients were plotted as a function of peak tube voltage and a logarithmic fit was used to calculate gradients for other peak tube voltages. This gradient characterized the relationship between variance and mean pixel intensity for a given beam energy. The gradient and the single offset made up the calibration model used by *simDR*.

2.1.2 *Adding simulated noise*

Computer-generated quantum noise was added to images frame by frame using pixel-to-pixel addition. The method applied was that described by Veldkamp et al.,[17] enhanced to incorporate the beam energy dependent calibration. First, the peak tube voltage used to acquire the input image was obtained from the image metadata and the calibration model was used to determine the relationship between pixel intensity and variance for the input image. The reduced dose image R was created by scaling the pixels' intensity values in the input image, I, by the amount q, and adding noise of the appropriate amount and color—the *mask*, described below. This is shown in Eq. (1) where q represents the ratio of the input image dose to the requested image dose. To calculate q, any input dose measurement or quantity proportional to dose can be used by the software (i.e., air kerma, entrance surface dose, x-ray tube current, and so on).

$$R = \frac{I}{q} + \text{mask}. \tag{1}$$

For a given image pixel intensity value the calibration model was used to calculate the variance σ^2_{input} in I and the variance $\sigma^2_{\text{lowdose}}$ required in R. The amount of variance to be added σ^2_{add} was then calculated as follows:[17]

$$\sigma^2_{\text{add}} = \sigma^2_{\text{input}} \frac{q^2 - P^2}{q^2 * P^2}, \tag{2}$$

where

$$P = \frac{\sqrt{\sigma^2_{\text{input}}}}{\sqrt{\sigma^2_{\text{lowdose}}}}. \tag{3}$$

A noise mask the same size as the input image was created. White noise was generated from a Poisson distribution of random numbers with specified (requested) variance σ^2_{add} divided by the correction factor (see below). The mean of this Poisson distribution was subtracted from the mask so that the white noise had a zero mean. The white noise was filtered by the normalized noise power spectrum (NPS) of the x-ray system, to color the white noise with accurate spatial frequency distribution of the variance i.e., noise texture. The square root of the NPS measured at a clinically-relevant dose was normalized by its zero frequency value to create the filter;[18] see Sec. 2.1.3 for a description of how this NPS was measured. The filtered noise mask was added to the scaled input image I/q to provide the reduced dose image R as shown in Eq. (1). Figure 1 shows an example frame of a white noise and filtered noise mask.

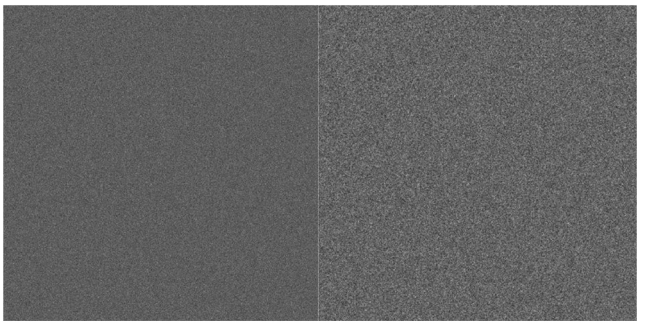

Fig. 1 Single frame from (a) a white noise mask and (b) filtered noise mask.

Filtering of white noise by the normalized NPS will have caused each pixel's variance in the final image to be reduced; a multiplicative correction applied to σ^2_{add} reversed these effects. To calculate this correction factor, the ratio of the variance of the filtered noise mask to the variance of the white noise mask was calculated for a range of dose values and the average value was used in *simDR*.

2.1.3 *Validation of noise simulation software*

SimDR was applied to every image sequence acquired above except for the ones with the lowest dose; standard deviation and signal-to-noise ratio (SNR) (i.e., mean pixel intensity divided by standard deviation) were calculated for each original and simulated flat field image sequence, using all frames. This was repeated for anthropomorphic phantom images. For the calculations a 685×685 pixel central region was used on the flat field images and four different small anatomic regions were used on the anthropomorphic phantom images (Fig. 2). Real and simulated image sequences representing the same input dose and beam energy were compared to test the noise simulation software.

For flat field images, NPS was calculated for each real and simulated sequence using bespoke NPS calculation software written in MATLAB®. The International Electrotechnical Commission (IEC) standard methodology for determination of detective quantum efficiency of dynamic digital x-ray image detectors was generally adhered to in terms of methods and materials; details not provided below can be found in the IEC document.[19] Radiation quality varied depending on the PMMA thickness and peak tube voltage which was used (see Table 1). The sensitivity (pixel intensity per detector entrance air kerma per frame) and the IEC-provided SNR^2_{in} for the corresponding radiation quality were used to convert image data from pixel intensity to quanta per mm^2. For image analysis, the first 10 frames were ignored to allow for temporal correlations in the image sequence to stabilize. The

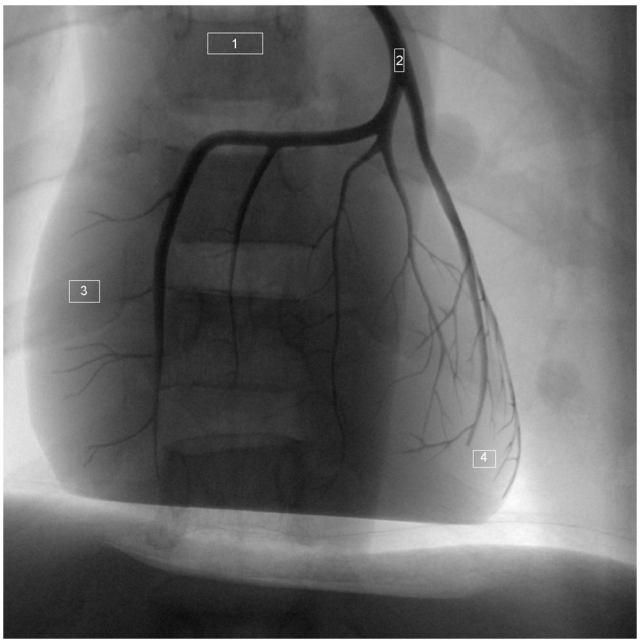

Fig. 2 Anthropomorphic phantom showing regions of interest (1 to 4): spine, iodinated vessel, rib, and airspace in the lung.

region of interest (ROI) size was 128×128 pixels with a 64 pixel overlap, chosen to provide a better trade-off between spatial frequency increment and susceptibility to noise in the analysis than the IEC recommended 256×256 pixel ROI. The NPS curves for real and simulated image sequences representing the same phantom ESDr were plotted on the same graph for visual comparison, using a 4th degree polynomial fit to smooth the curves.

When calculating the NPS for coloring the white noise (Sec. 2.1.1), the only differences in methodology from above were the use of radiation quality RQA 5 (70 kVp, 21 mm Al, no PMMA) and a 110 cm SID; the detector entrance air kerma was 173 nGy, as used in angiography.

Images of an anthropomorphic chest phantom containing contrast-filled coronary arteries (Radiology Support Devices Alderson Phantoms, Long Beach) were obtained using the experimental setup described in Sec. 2.1.1. Peak tube voltages of 65 and 80 kVp were used with 100 cm SID, for a range of dose levels. Radiographic factors and ESDr are shown in Tables 6 and 7 (in Sec. 3). Four anatomical regions including the spine, iodinated vessel, rib, and airspace in the lung were selected as shown in Fig. 2. Figure 3 shows an example of a simulated low-dose anthropomorphic phantom image frame, including the original and simulated 81% dose reduction images and corresponding real low-dose image for visual comparison; no post processing was applied.

In order to validate the software by subjective image assessment, real and simulated images of a threshold contrast detail detectability (TCDD) phantom representing the same input dose and beam energy were judged by three observers and the results were compared. Manufactured by the research group, this phantom is an original prototype of a widely-used, commercially-available threshold contrast phantom (TO10, Leeds Test Objects, Borough Bridge, UK). It is standard practice for hospital physicists to utilize this phantom for routine testing of interventional x-ray imaging equipment,[20] hence it was the most appropriate phantom for this task. The 6-cm thick PMMA test object has 12 rows of embedded metal disc shaped details, with each row comprising discs of a smaller diameter than the previous row. Each row has details of calibrated, decreasing subject contrast and depending on the x-ray settings, not all details in each row are visible.[21,22]

Raw TCDD image data was captured using the experimental set up described in Sec. 2.1.1, except with the phantom taped to the outside surface of the antiscatter grid. A peak tube voltage of 75 kVp was used with 1.5 mm copper filtration added, as is standard practice.[23] Air kerma was measured 60.5 cm from the x-ray source, and inverse square law corrected to calculate the detector input air kerma, the dose measurement used when implementing the noise simulation software on the TCDD images. Radiographic factors and detector air kerma measurements are shown in Table 2; the three highest dose image sequences in Table 2 were used to create simulated image sequences of the other four dose

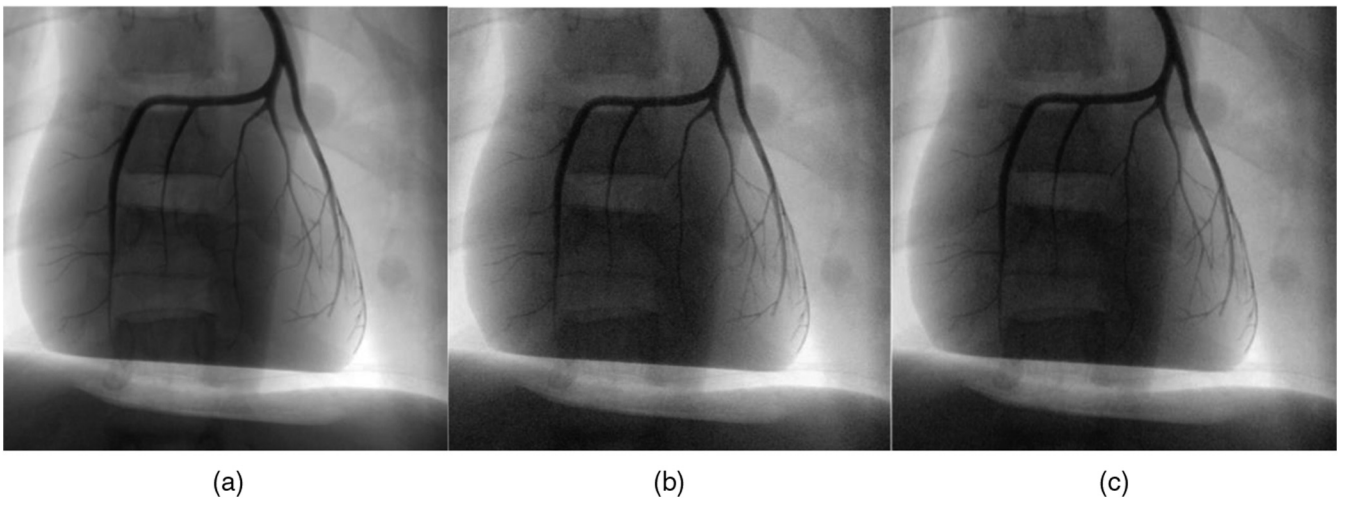

Fig. 3 (a) Original anthropomorphic phantom image frame, (b) simulated image of original with 81% dose reduction, and (c) real image with the same input dose as the simulated image. For display, a log look-up table was applied and images were scaled by MATLAB®.

Table 2 Radiographic factors and detector air kerma per frame used for threshold contrast detail detectability (TCDD) study with simulated dose reduction.

Peak tube voltage (kVps)	Peak tube current (mA)	Pulse duration (ms)	Detector air kerma (nGy/frame)	Simulated dose reduction (%)	
75	85	5	36	77	57
75	120	5	54	75	46
75	170	5	85	78	46
75	200	5	101	74	54
75	300	5	157		
75	400	5	218		
75	700	5	389		

levels, and were not included in the subjective validation. Both 50% and 80% (approximately) dose reduction were simulated using the software, for comparison with real image sequences acquired with same detector input air kerma. Figure 4 shows an example TCDD phantom image frame, including the original and simulated 75% dose reduction images and corresponding real low-dose image for visual comparison; no post processing was applied.

Three experienced medical physicists (first, third, and final authors) viewed in randomized order simulated and real image sequences with detector air kerma rates of 36, 54, 85, and 101 nGy/frame, recording the number of visible contrast details in each row of the phantom. Image sequences of 960×960 pixels were displayed at 15 frames/s with an 8-bit depth, using a medical grade monitor 70 cm from the observer with dimmed ambient lighting. More monitor details are provided in Sec. 2.2.2. The preprocessing logarithmic pixel transformation look-up table which had been reversed for image data linearity (see Sec. 2.1.1) was reapplied for viewing, and images were automatically scaled in MATLAB®. No time restrictions were enforced. Contrast scores were averaged between observers. For each row, scores were converted into visible contrast threshold, $C_T(A)$, where A is the area of the disk detail; these were then averaged for each row, as per standard practice,[20–23] and results were presented as a derivative parameter—detection index, $H_T(A)$, [see Eq. (4)]—which is inversely proportional to contrast threshold.

$$H_T(A) = [C_T(A)\sqrt{A}]^{-1}. \tag{4}$$

2.2 *Image Assessment*

2.2.1 *Adding noise to patient images*

Patient images were acquired on the same Allura Xper cardiac x-ray system at Yorkshire Heart Centre, Leeds, as referred to in Sec. 2.1. For research purposes, the system was modified to allow for image capture prior to enhancement that is normally applied to clinical images, as described in Sec. 2.1.1. The same digital ("cine") acquisition mode was used to capture images, at 15 frames/s, with the antiscatter grid in place—as per normal clinical practice for angiography. Angiograms used in this study were selected from routine PCI procedures of five different cardiac patients; five was deemed enough for a feasibility study provided the images represented the range of patient sizes. These five angiograms were specifically selected to represent the range of adult cardiac patient sizes (body mass index 23 to 44 $\mathrm{kg\,m^{-2}}$ and to include angular cardiac views—of both the left and right coronary arteries—commonly used in clinical practice (see Table 3); x-ray settings required to create an image are highly dependent on these selection criteria. The patient images were anonymized and their use for this study was approved by the National Health Service Research Ethics Committee.

Increments of computer-generated quantum noise were added to patient images using *simDR* to simulate corresponding increments of dose reduction. For each patient image, the result was a large collection of different versions of that

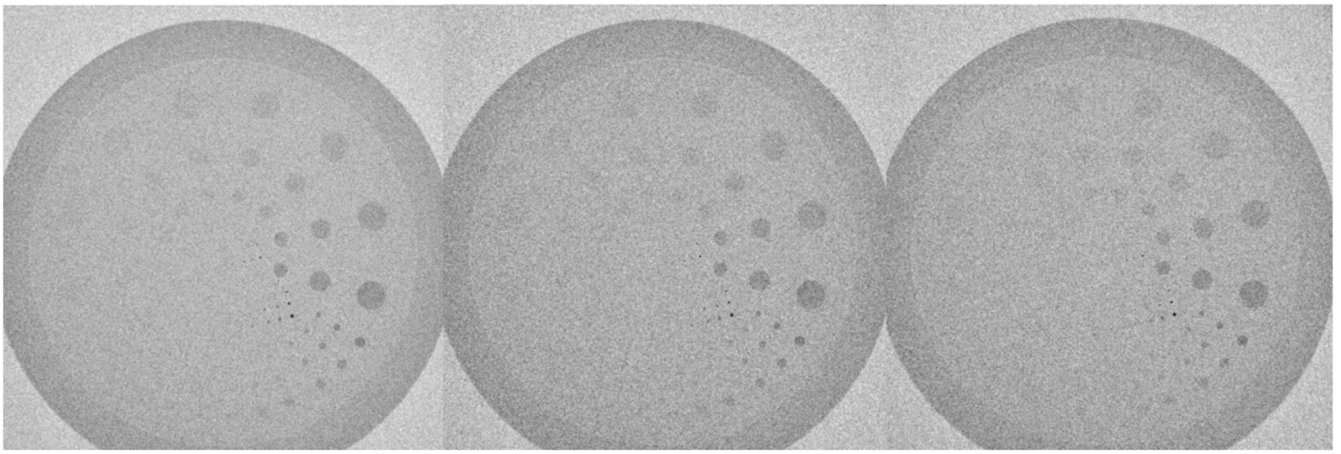

Fig. 4 (a) Original threshold contrast detail detectability phantom image frame, (b) simulated image of original with 50% dose reduction, and (c) real image with the same input dose as the simulated image. For display, a log look-up table was applied and images were scaled by MATLAB®.

Table 3 Patient image details and patient body mass index (BMI); right and left anterior oblique angles are RAO and LAO, respectively.

Patient number	BMI ($kg\,m^{-2}$)	Vessel of interest	C-arm rotation (deg)	C-arm angulation (deg)
1	25.6	Circumflex (left)	RAO 90	Caudal 3
2	44.1	Right coronary artery	RAO 35	Caudal 17
3	29.4	Left anterior descending artery	LAO 37	Caudal 31
4	36.5	Left anterior descending artery	RAO 3	Caudal 20
5	23.8	Right coronary artery	LAO 28	Cranial 1

image—representing 1%, in integer increments, to 99% dose reduction with respect to the original dose at which the angiogram was captured on the x-ray system; these required 26.3 GB of memory space to store. Figure 5 shows two examples (patient numbers 2 and 4 from Table 3); on the left hand side is an image frame from the original angiogram as acquired on the x-ray system during the PCI procedure. On the right hand side is the image frame with noise added to simulate 60% dose reduction with respect to the original angiogram.

2.2.2 *Image viewing sessions*

Images were viewed on a 10-bit DICOM-calibrated RadiForce RX340 medical grade monitor (EIZO Corporation, Ishikawa, Japan) in the radiology viewing room at Yorkshire Heart Centre, with placement of the monitor 1 m away to simulate an interventional laboratory. The ambient light in this room was slightly dimmed, as per standard angiogram viewing.

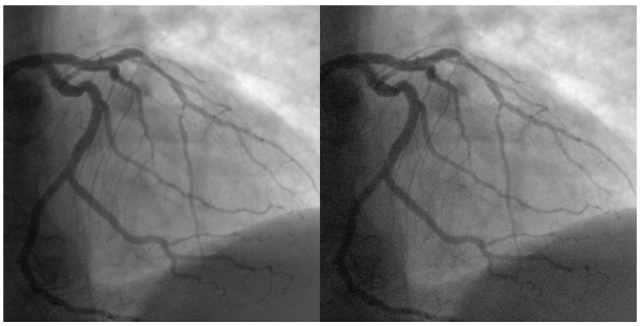

(a)

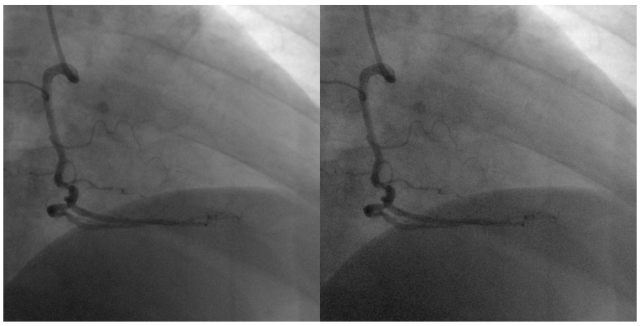

(b)

Fig. 5 Single image frame from (left) original and (right) degraded angiogram to represent 60% dose reduction for patient number (a) 2 and (b) 4.

Calibration was performed automatically prior to this study such that the monitor was perceptually linear. Twelve observers—five experienced radiographers working in the cardiac catheter labs and seven interventional cardiologists (see Table 4 for years' experience)—each viewed all five patient angiograms, for 60 total observations. The 960×960 pixel angiograms were viewed at 15 frames/s, at an 8-bit depth, in a proprietary format. The preprocessing logarithmic pixel transformation look-up table which had been reversed for image data linearity (see Sec. 2.1.1) was reapplied for viewing, and images were automatically scaled in MATLAB®. Ethical approval for the observer study was granted by the University of Leeds Research Ethics Committee and the National Health Service Research and Development Department.

A second bespoke software program dynamic X-Ray Image Perception Measurement (*dXRIPM*) was written in MATLAB® to run the viewing sessions and determine the observers' perception of image degradation. A DELL

Table 4 Years' experience with angiography/interventional procedures for each study observer, with clinical role.

Years' experience	Clinical role
20	Interventional cardiologist/Radiologist
22	Radiographer
22	Radiographer
15	Radiographer
14	Radiographer
30	Radiographer
5	Interventional cardiologist
15	Interventional cardiologist
8	Interventional cardiologist
7	Interventional cardiologist
35	Interventional cardiologist
5	Interventional cardiologist

Optiplex 760 personal computer with 8 GB of memory and an Intel Core Duo processor was used; the preprepared patient images of multiple dose levels were read on-the-fly by *dXRIPM* as required. The software executed an established psychophysics experimental method which was adapted to measure perception of the x-ray images of blood flowing through the heart. The experimental design, called a "staircase" or "transformed up/down" psychophysics experiment,[24] was selected because it has been shown to maximize efficiency of observer perception tests such as the one required for this study.[25,26] The original (standard radiation dose) and degraded images (simulating lower radiation dose) of the same patient were shown side by side as an image pair, with left and right placement of images in the pair randomized. Observers were asked to focus their attention on the clarity with which the coronary arteries of the heart were shown, answering the question "which side [left or right, in the image pair] shows the arteries more clearly?" in a two alternative forced choice (2AFC) test. The angiograms looped synchronously and continuously until the observer made a decision; no time limit was imposed. Once the observer selected the preferred image (using the left or right arrows on the keyboard), *dXRIPM* showed the next image pair based on the selection which was made.

A high level of degradation was set (60% dose reduction) for the first few image pairs, making the difference between the left and right images apparent. These relatively easy decisions allowed for a period of training for the observers to develop confidence and become comfortable with the process,[24] and results from training images were not used for data analysis. The 1 up/3 down rule[26] was used following training: when an observer chose the original image three consecutive times (three "correct" responses, as the original had no noise added), the level of degradation was reduced in the next image pair—a step down; when the observer chose the degraded image one time (an "incorrect" answer as the degraded image had noise added), the level of degradation was increased in the next image pair—a step up. The degree of degradation (size of step) decreased after each reversal in step direction to maximize accuracy and efficiency of the staircase experiment.[27]

A level of degradation was eventually reached where the observer had difficulty deciding between the original and degraded image, indicating that the degradation was no longer perceived. Using the still frames in Fig. 5 as an example, the degradation in the right hand image was reduced until the left and right hand images looked the same. Because it was a 2AFC test, i.e., the observer could not state that both images were the same, the steps then went up and down in degradation level as the observer was forced to choose either the left image or the right image. Several reversals in direction around a certain degradation level represented the observers' inability to consistently make decisions at that level. The mean of the reversal points was the level of

Table 5 Left to right: flat field image capture data (peak tube voltage and current, pulse duration, entrance surface dose rate), dose reduction simulated and results (signal to noise ratio and standard deviation) with percent difference between real and simulated image measurements.

Peak tube voltage, tube current, x-ray pulse duration (kVp, mA, ms)	Entrance surface dose rate (mGy/s)	Dose reduced by (%)	Real SNR	Real SD	*Sim* SNR	*Sim* SD	%Dif SNR	%Dif SD
69, 400, 5	1.3	67	17	39	*18*	*39*	**4.5**	**0.4**
69, 500, 5	1.7	58	20	43	*20*	*44*	**2.4**	**0.3**
69, 600, 5	2.0	49	22	47	*22*	*48*	**2.1**	**0.6**
69, 600, 10	4.0		31	67				
75, 600, 6	3.1	63	16	38	*16*	*38*	**2.5**	**1.7**
75, 800, 6	4.1	50	18	44	*19*	*43*	**4.0**	**1.4**
75, 800, 12	8.3		27	62				
92, 500, 8	5.9	52	15	42	*16*	*41*	**4.4**	**1.0**
92, 700, 8	8.3	33	18	49	*19*	*49*	**1.2**	**0.8**
92, 700, 12	12.4		23	60				
118, 300, 10	8.0	47	12	38	*13*	*37*	**4.1**	**2.1**
118, 400, 10	10.8	29	14	44	*14*	*43*	**3.3**	**1.6**
118, 500, 10	13.4	12	16	49	*16*	*48*	**1.7**	**2.1**
118, 565, 10	15.2		17	52				

Table 6 Left to right: Anthropomorphic phantom image capture (peak tube voltage and current, pulse duration, entrance surface dose rate), dose reduction simulated and results (signal to noise ratio and standard deviation) with percent difference between real and simulated image measurements (65 kVp).

Peak tube voltage, tube current, x-ray pulse duration (kVp, mA, ms)	Entrance surface dose rate (mGy/s)	Dose reduced by (%)	Region of interest	Real SNR	Real SD	*Sim* SNR	*Sim* SD	%Dif SNR	%Dif SD
65, 400, 5	0.92	75	Spine	21	45	*21*	*44*	**0.9**	**0.9**
			Vessel	21	44	*21*	*43*	**1.2**	**1.3**
			Rib	21	51	*21*	*49*	**0.8**	**2.8**
			Lung	26	59	*26*	*58*	**1.0**	**2.3**
65, 500, 5	1.17	63	Spine	24	49	*24*	*49*	**0.3**	**1.1**
			Vessel	23	51	*24*	*49*	**0.0**	**2.3**
			Rib	24	57	*24*	*55*	**0.6**	**1.8**
			Lung	31	64	*30*	*65*	**0.2**	**3.6**
65, 600, 5	1.39	50	Spine	26	55	*26*	*53*	**0.3**	**0.6**
			Vessel	26	55	*26*	*53*	**0.9**	**0.1**
			Rib	26	63	*26*	*61*	**0.1**	**1.4**
			Lung	32	73	*32*	*72*	**0.4**	**1.5**
65, 800, 5	1.86		Spine	30	63				
			Vessel	30	62				
			Rib	30	72				
			Lung	37	171				

degradation no longer perceived by the observer; this is known as the threshold or point of subjective equality (PSE), and was calculated by *dXRIPM*.

During one viewing session, the five staircase experiments were interleaved at random, i.e., *dXRIPM* randomly selected which angiogram would be shown next. Each individual staircase terminated when the precision of the PSE calculation was below a set amount or the observer had viewed fifty image pairs.

2.2.3 *Statistical analyses*

Prior to the above viewing sessions, a pilot study was completed for a sample size (power) calculation—to determine how many observations would be required to make conclusions that were statistically acceptable. Thirteen observers working in the field of medical imaging each viewed between two and four patients, depending on their time available, for 25 total observations. Altman's nomogram showed that 60 observations were required for this study to achieve 80% power at 5% statistical significance.

Median values of PSE were calculated with the first and third quartiles, minimum and maximum values, per patient and for the selected patient population. For each patient's PSE, the correlation between years' experience of the observer and PSE were determined using a Pearson's correlation coefficient.

3 Results

3.1 *Validation of Noise Simulation Software*

Standard deviation and SNR, with corresponding percentage differences between real and simulated flat field images, are shown in Tables 5, 6, and 7 for flat field and anthropomorphic phantom images; differences were all less than 5%. For brevity, only simulated images created using the largest dose image, for up to 75% dose reduction, are included; accuracy was consistent regardless of the input image dose level.

The NPS curves were well matched in all cases, and two examples are shown in Fig. 6 for 30% and 75% dose reduction at 69 and 118 kVp, respectively. Results from the subjective validation are shown in Table 8. The research group previously found a relative standard error of up to 10%[21] in the methods used hence 10% relative errors are shown. For a given detector input air kerma, differences in detection indices were all within error (all except one measurement were within 5% agreement); therefore, there was no statistically

Table 7 Left to right: Anthropomorphic phantom image capture data (peak tube voltage and current, pulse duration, entrance surface dose rate), dose reduction simulated and results (signal to noise ratio and standard deviation) with percent difference between real and simulated image measurements (80 kVp).

Peak tube voltage, tube current, x-ray pulse duration (kVp, mA, ms)	Entrance surface dose rate (mGy/s)	Dose reduced by (%)	Region of interest	Real SNR	Real SD	*Sim* SNR	*Sim* SD	%Dif SNR	%Dif SD
80, 200, 5	0.85	76	Spine	26	61	*25*	*62*	**0.2**	**3.4**
			Vessel	26	63	*26*	*63*	**1.1**	**3.2**
			Rib	25	69	*26*	*67*	**5.6**	**1.9**
			Lung	30	80	*31*	*79*	**4.2**	**0.8**
80, 400, 5	1.73	51	Spine	37	87	*37*	*89*	**1.3**	**2.1**
			Vessel	38	90	*37*	*91*	**1.2**	**1.2**
			Rib	36	101	*37*	*99*	**2.9**	**1.9**
			Lung	43	117	*44*	*114*	**2.1**	**1.2**
80, 600, 5	2.62	26	Spine	45	110	*45*	*110*	**0.3**	**0.3**
			Vessel	46	112	*46*	*112*	**0.5**	**0.1**
			Rib	44	126	*45*	*124*	**1.4**	**1.4**
			Lung	52	147	*53*	*144*	**1.4**	**1.3**
80, 800, 5	3.53		Spine	52	128				
			Vessel	53	131				
			Rib	51	147				
			Lung	60	171				

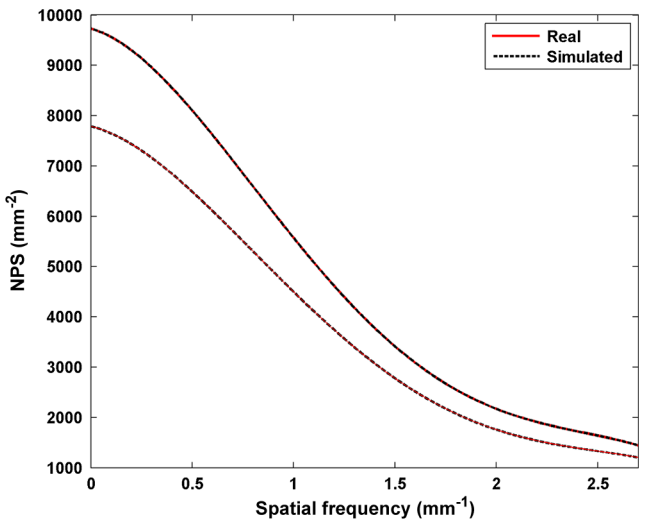

Fig. 6 Noise power spectra for (bottom curves) entrance surface dose rate 1.3 mGy s^{-1} at 69 kVp with 75% dose reduction and (top curves) 10.8 mGy s^{-1} at 118 kVp with 29% dose reduction.

significant difference between real and simulated results for both levels of dose reduction, independent of the input image dose level.

3.2 *Image Assessment*

The median PSE $\pm$ standard deviation for the five PCI patients was 33% $\pm$ 15% dose reduction. The PSEs for the five patients ranged from 25% to 48% dose reduction,

Table 8 Contrast detection index $H_T(A)$ as a function of detector input air kerma for real and simulated (50% and 80%) images representing the same dose with error range as [min, max]

Air kerma (nGy/frame)	Real	Simulated 50%	Simulated 80%
101	9.02 [8.12, 9.92]	8.58 [7.72, 9.44]	8.92 [8.03, 9.81]
85	7.95 [7.16, 8.75]	8.16 [7.34, 8.97]	7.88 [7.09, 8.67]
54	6.83 [6.15, 7.52]	6.43 [5.79, 7.07]	6.88 [6.19, 7.57]
36	5.75 [5.18, 6.33]	5.57 [5.01, 6.12]	5.59 [5.03, 6.15]

reflecting the wide range of patient BMIs and projection angles included in the study. The PSEs are shown for each patient in Fig. 7 and for the patient population in Fig. 8; median values are shown as long lines, first and third quartiles as boxes, minimum and maximum values as short lines, and outliers as plus signs. There was no statistically significant correlation found between the number of years' experience of the observers and their PSEs.

A variety of staircase shapes were found, as demonstrated by the three examples shown in Fig. 9; the dotted line represents the PSE. The green dots represent "correct" responses (original angiogram chosen) and the red dots represent "incorrect" responses (degraded angiogram chosen); the X's represent a reversal in direction. The standard deviations for most of the 60 calculated PSEs, i.e., precision in the measurements were below 10% dose reduction; three had a precision of 11% to 15% dose reduction.

4 Discussion

This research used PCI patient images to quantify how much image noise could be added in cardiac x-ray imaging without loss in perceived image quality, and the amount was not negligible. Results indicate that a significant ($33\% \pm 15\%$) reduction in radiation dose used for PCI procedures may be feasible without compromising patient care. The lowest feasible dose reduction is 18%, indicating that the quality of cardiac x-ray images may be systematically too high, as suggested by Dixon and Wagner.[14]

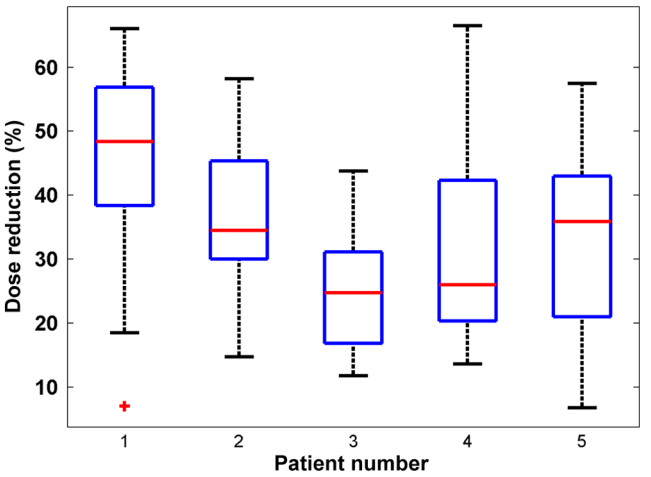

Fig. 7 Points of subjective equality for each patient angiogram shown in % dose reduction: median (long line), first and third quartiles (box), minimum and maximum (short lines), and outliers (+'s).

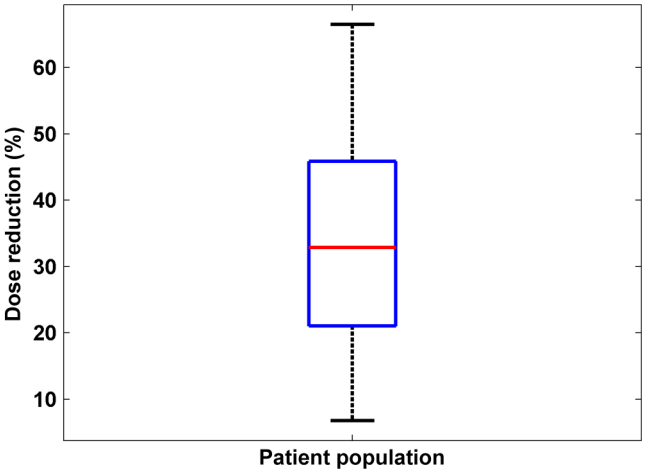

Fig. 8 Point of subjective equality for the five patient angiograms, shown in % dose reduction: median (long line), first and third quartiles (box), minimum and maximum (short lines).

It is not feasible to manually change x-ray settings on the imaging system during a patient procedure, i.e., lowering dose until an appropriate level of image quality is reached. This is due to the closed-loop, "black-box" nature of the ADRC used to control the settings on these x-ray systems;[16] only specific manufacturer engineers have access to settings. In order for manufacturers to change clinical imaging protocol to reduce dose, a strong case of evidence for such a change must be made; this could be achieved using the off-line analysis method presented in this study, pending results of a future larger-scale study (see Sec. 4.2).

Experienced radiographers working in the cardiac interventional lab were recruited as observers in addition to cardiologists, as per recommendations from cardiologists. With the radiographers' results removed from the statistical analysis, the median PSE$\pm$ standard deviation for the five PCI patients was $36\% \pm 14\%$ dose reduction; the difference between these and the study results was not statistically significant. This demonstrates that recruiting both clinical professions was suitable for the study. Cardiologists reported that compared to image assessments which involve scoring, this type of experiment was relatively easy to complete. Five interleaved staircase experiments were completed in an average time of 35 min.

The use of patient images at multiple dose levels was made possible with the *simDR* software, which was calibrated and validated using unenhanced image data from a specific image acquisition mode on the Philips Allura Xper cardiac interventional x-ray system. For a different imaging mode or a different x-ray system, *simDR* calibration and validation procedures would need to be repeated using unenhanced image data from that mode or x-ray system, in order to accurately simulate dose reduction. This study was made possible because the manufacturer provided the means to linearize the image data, i.e., make the pixel intensity proportional to the dose, and a means of capturing unenhanced image data. Others wishing to repeat the procedure should be aware that this is required to accurately calibrate the software and add noise to patient images.

The TCDD phantom used to subjectively validate *SimDR* lacks dynamic or clinically-relevant content, however, it was selected for validation because it is a well-known, standard phantom used by hospital physicists in the UK[20] and worldwide[28] to assess cardiac x-ray system image quality. The contrast detection index is a well-understood measurement within the industry, as is the procedure of assessing the images and extracting this measurement. The authors recognize the lack of a more clinically-relevant, dynamic phantom for assessing image quality of cardiac x-ray systems. The intention of this feasibility study was to address this issue; the purpose of developing *SimDR* was to allow for clinically-relevant image quality assessments to be completed using dynamic patient images.

In validating *simDR*, the noise measurements performed on simulated low-dose images varied slightly in value each

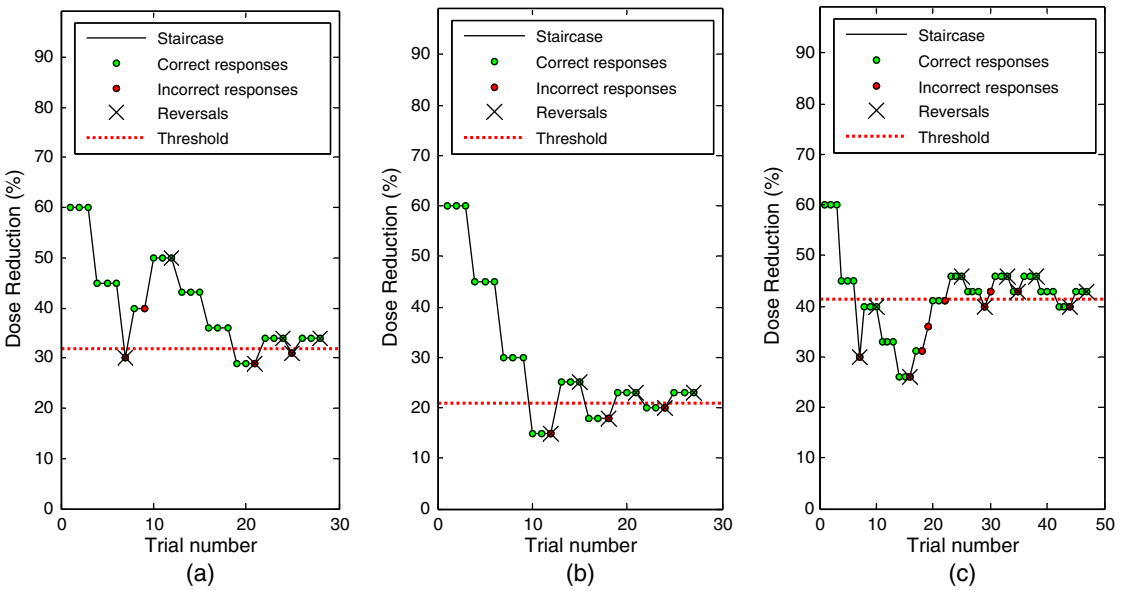

Fig. 9 (a)–(c) Three example staircase results; the threshold denoted by the dotted line is the point of subjective equality.

time they were repeated due to the use of random noise; standard error in these measurements was much less than 1%. Measurements also varied from frame to frame due to variations within an image sequence; values may have differed should longer or shorter image sequences have been used. All the phantom image sequences were the same length for consistency.

The NPS filter colored the white noise very accurately, providing well matched curves for NPS comparisons while maintaining accurate measures of noise in the spatial domain. The authors had previously filtered the white noise by the modulation transfer function (MTF) of the detector; simulated and real low-dose standard deviations were within 10% agreement and corresponding TCDD phantom images appeared the same (similar results to above), however, NPS curve shapes were not well matched. The curves crossed over each other between 1 and 2 mm^{-1}, depending on the ESDr, with the simulated spectra too high at low-spatial frequencies and too low at high-spatial frequencies. The difference in spectra at 0 nm^{-1} was up to 30%, depending on the dose. This demonstrates the importance of examining the noise texture, and not only spatial domain measurements, in order to thoroughly check the software for accuracy. The difference in NPS comparisons having used an MTF filter compared to those from using an NPS filter may be explained by aliasing from digital sampling.[29] In addition, it suggests that nonquantum noise sources are subject to the MTF of the detector in a different (likely dose dependent) manner than is the quantum noise. It follows that by using the NPS filter to color the noise, nonquantum noise sources were sufficiently accounted for in this study.

The method used here to simulate dose reduction is not the only method of patient dose reduction which is possible; it is simply the one which was chosen for this study. Moreover, patient dose (skin or effective) is not linearly related to the input radiation dose at the detector.

4.1 *Comparison with Past Studies*

In other x-ray imaging applications, computer processing of clinical images to produce images representative of those acquired at a lower dose through adding simulated image noise is a useful tool which helps overcome the ethical issue of multiple exposures of the same patient at each dose level to be studied. Noise simulation software has been developed for use mainly in computed tomography (CT)[30–34] and digital radiography[17,18,35,36] applications, as well as mammography[37] and tomosynthesis.[38] There is no such published tool for cardiac x-ray imaging to date, to the authors' knowledge. All of these published techniques utilized one x-ray beam energy for the imaging mode in question. This is practical for some x-ray modalities, for example, 120 kVp for CT of the brain,[31] 28 kVp for low-dose mammography[37] and 133 kVp for chest radiography.[17] In cardiac x-ray imaging, the peak tube voltage is controlled by ADRC, changing with different patient sizes and different projections angles; manufacturers differ in their ADRC design.[39] Therefore, in order for a dose reduction simulation technique to be useful for cardiac x-ray imaging, it must address the full range of peak tube voltage values which may be set by the system. *SimDR* is unique in that it is the first published dose reduction simulation technique to address the full range of x-ray tube voltages which may be used in clinical practice. Söderberg et al. [32] created a tool for use in CT over a range of x-ray tube voltages, however, the software did not work for transverse slice images captured at lower tube voltages, i.e., less penetrating x-ray beams.

The method for noise simulation used in this study was adapted from Veldkamp et al.[17] and Saunders and Samei[18]—both DR studies—for variance calculation and NPS filtering of the noise mask, respectively. Veldkamp et al. did not filter their white noise mask to account for the spatial frequency distribution of the system noise, and they had similar disagreement in real and simulated image NPS as this study found using MTF rather than NPS as the white noise filter.

Saunders and Samei, like the current study, had excellent NPS agreement. Other studies showed a mix of very good[32,33,38] and poor[35,36] agreement between real and simulated image NPS. Only some past studies evaluated images subjectively, and a range of diverse methods were used, depending on the x-ray imaging modality and the clinical task.[17,30,31,34,35,37]

In past investigations seeking to optimize radiation dose with image quality for cardiac x-ray imaging, physicists have utilized technical measurements of image quality from static phantom-based experiments.[40–42] Results from these studies reported optimal x-ray settings, therefore, results cannot be compared with the current study. According to the literature the method utilized in this study has not been applied to cardiac x-ray imaging, most likely because image degradation software to simulate changes in dose had not been developed. A further barrier—in addition to taking into account a range of beam energies—preventing the development of such software is the requirement to operate on images prior to application of any image enhancement (processing); these images are not normally available to end users.

The method utilized in this study has, however, been applied to CT. Frush et al.[30] added noise to pediatric abdominal CT images to simulate dose reduction, and found that dose could be reduced by 33% to 67% depending on whether low or high-visibility structures were sought. Britten et al.[31] similarly found that dose could be halved for brain CT while still allowing for identification of periventricular low-density lesions. In these studies, images were assessed by three and two radiologists, respectively; conversely the current study performed a power calculation using a pilot study to ensure that a sufficient number of observations took place.

The 2AFC methodology used in this study is sometimes referred to as a "matched" or "paired-comparison" study. There are no prior publications of using 2AFC with a transformed 1 up/3 down staircase using patient angiograms, however, a paired-comparison was used in a high-impact study which established the importance of viewing image sequences rather than "last image hold" frames when evaluating dynamic x-ray systems.[43] This study experimentally demonstrated that the temporal filtering in the human visual system reduces perceived noise; the authors demonstrated in this and another study[44] that paired-comparison is more reliable than minimum contrast (detectability) measurements, and that their measured "equivalent perception dose" depends upon the shape and size of the phantom's contrast detail. This supports the current study methodology in two ways—the use of 2AFC and the independence of results on contrast detail since it used clinically-relevant (patient) images.

The same research group explored the impact of image enhancement technologies[45–47] and changes in frame rates[44,48] on perceived image quality for dynamic x-ray systems, reporting in some cases a potential to reduce dose. Wilson et al.[47] utilized an adaptive, 9AFC low-contrast detectability study to show that temporal noise reduction filtering is not perceived. They found that a technical measurement of displayed noise is not an adequate assessment of image quality because it does not take into consideration the human visual system. The current study supports these conclusions despite the study design differences: The current study was adaptive, however, it showed angiograms with only two alternatives; Wilson et al.[47] note that 9AFC and 2AFC ("paired-comparison") studies are not the same. In addition, the current study did not investigate image enhancement algorithms or frame rates. The major difference between the current study and the work of the other research group is that they measure perception of contrast-detail based phantoms, aside from one 4AFC evaluation of a stent-based phantom,[49] whereas the current study utilizes patient image sequences. For the current study, detectability was not of interest because angiography (digital "cine" acquisition mode) rather than fluoroscopy was investigated. In angiography, the vessels must be higher than just-detectable, whereas in fluoroscopy contrast detail detectability is more clinically-relevant with respect to locating catheter tips, balloon markers, etc. In this capacity, the current study is complementary to these past studies.

4.2 *Potential Impact and Future Work*

Measuring the quality of x-ray images is not straight forward. Technical aspects of image quality (such as noise), often produced by computer analysis of static phantom or test object images, are reproducible and can provide excellent means of analyzing the performance of x-ray system components. However, it is not possible to translate technical measurements into the imaging of human subjects (patients). The utility of cardiac patient x-ray images is in their interpretation by a cardiologist during an interventional procedure, and it is not well understood how changes in technical image quality are perceived by a clinician.[50,51] This issue was investigated by Tingberg et al.[52] who, using a screen-film x-ray system, degraded images to simulate changes in two different x-ray system settings; lumbar spine radiographs were scored by radiologists to determine which of the two corresponding technical measurements was of greater clinical importance. Saunders and Samei[18] developed image degradation software to simulate changes in x-ray settings on a digital radiography x-ray system as their first step to address this issue. The findings presented here represent another step toward understanding the relationship between technical measurements and clinical image perception. Using image degradation software to simulate changes in dose on a cardiac x-ray system, the amount of noise which can be added to a patient image without being perceived by a clinician has been quantified.

This understanding of how changes in noise are perceived by clinicians may also help inform the design of future interventional (dynamic) x-ray systems, where x-ray settings are controlled automatically by specially-designed ADRC mechanisms. During a clinical procedure, this mechanism allows for hands-free operation, ensuring adequate image quality is maintained with an acceptable radiation dose to the patient. Currently, commonplace ADRC designs quantify image quality by performing a simple technical measurement directly from the image.[16,39] If image quality is set too high, unnecessarily high levels of x-ray dose are used. A more intelligent dose control design[53] would utilize a clinically-relevant measure of image quality as part of the automated mechanism; i.e., image perception by a cardiologist should be considered in the design of ADRC, to ascertain the required level of image quality to preset the dose control. This study has provided a preliminary step in designing an intelligent dose control mechanism. Understanding how changes in image contrast (i.e., changes in x-ray beam energy)

are perceived would be the next step. Should a method be devised to accurately simulate changes in beam energy, the *dXRIPM* software could be used to measure perception for such future work.

Digital image enhancement normally used in cardiac interventional x-ray labs may impact the PSE should this staircase experiment be repeated using enhanced images. The collection of patient angiograms over a range of dose levels would need to be processed by the manufacturer's clinical image enhancement algorithm. This future work, using a larger sample of the patient population and a greater number of observers, would be required in order to make a case for clinical implementation of study conclusions, i.e., reduce the dose by 33%. Clinical implementation of study conclusions would entail changing clinical protocol by reprogramming x-ray settings (dose control). By reducing the radiation dose used for interventional cardiac procedures, patient exposure would decrease, as would the occurrence of hair loss and skin burns; this could, in turn, reduce the need for skin grafts with these patients. Risk of cancer later in life could be reduced for pediatric patients—most of whom have genetic heart defects and require repeated procedures.[54] Reducing dose could also lead to reduced incidence of cancer and cataracts for interventional cardiologists.

This study investigated dose reduction in angiography for PCI patients. Fluoroscopy mode was not investigated; this would necessitate repeating the *simDR* calibration and validation processes using fluoroscopy image sequences. This noise simulation software was developed for dose optimization purposes, and fluoroscopy doses being lower than those of angiography, reducing fluoroscopy dose levels was not as high a priority as reducing angiography dose levels for cardiac interventional x-ray imaging. This study design, including both software programs, may be applied to fluoroscopy mode and to other cardiac interventional x-ray imaging procedures such as electrophysiology and trans-catheter aortic valve implantation.

5 Conclusions

The method presented for simulating dose reduction in cardiac interventional x-ray imaging by adding quantum image noise has been successfully validated by objective and subjective measurements. Standard deviation and noise power spectra, that is the amount and spatial frequency distribution of noise, as well as the SNR for real and simulated images representing the same input dose and beam energy were within 5% agreement for up to 75% simulated dose reduction. Differences between subjective evaluations of real and simulated images were within the error associated with the measurement, demonstrating no statistically significant differences.

The noise simulation software described can produce accurate low-dose images, and has been applied to five PCI patient angiograms to determine the feasibility of a clinically-relevant dose optimization experiment without irradiating patients. The results demonstrated the scope to increase noise of cardiac x-ray images by $33\% \pm 15\%$ before it is noticeable by clinical professionals, indicating a potential for $33\% \pm 15\%$ dose reduction without compromising patient care. If this dose reduction were implemented in clinical practice, both patients and clinical personnel would receive health benefits.

By quantifying the perception of quantum noise in cardiac x-ray imaging, this study will help support a movement toward understanding the relationship between technical image quality measurements and clinical image perception. This information could in turn help inform an intelligent dose control mechanism on future cardiac interventional x-ray systems.

Acknowledgments

This work was funded in part by Philips Healthcare, the Netherlands. Part of this work has been performed in the project PANORAMA, co-funded by grants from Belgium, Italy, France, the Netherlands, and the United Kingdom, and the ENIAC Joint Undertaking. The authors would like to acknowledge Claire Keeble and Paul Baxter from the University of Leeds Division of Epidemiology and Biostatics for their support on statistical analysis, as well as Ivana Kaljevic for her contribution to developing the noise simulation software. Thanks to all the observers who took part in the study (and pilot study).

References

1. J. A. Finegold, P. Asaria, and D. P. Francis, "Mortality from ischaemic heart disease by country, region, and age: statistics from World Health Organisation and United Nations," *Int. J. Cardiol.* **168**(2), 934–945 (2013).
2. D. Bor, "Comparison of effective doses obtained from dose-area product and air kerma measurements in interventional radiology," *Br. J. Radiol.* **77**(916), 315–322 (2004).
3. R. E. Vlietstra et al., "Radiation burns as a severe complication of fluoroscopically guided cardiological interventions," *J. Interventional Cardiol.* **17**(3), 131–142 (2004).
4. T. H. Frazier et al., "Fluoroscopy-induced chronic radiation skin injury: a disease perhaps often overlooked," *Arch. Dermatol.* **143**(5), 637–640 (2007).
5. M. F. Henry et al., "Fluoroscopy-induced chronic radiation dermatitis: a report of three cases," *Dermatol. Online J.* **15**(1), 1–5 (2009).
6. S. Balter et al., "Fluoroscopically guided interventional procedures: a review of radiation effects on patients' skin and hair," *Radiology* **254**(2), 326–341 (2010).
7. Icrp, "P103: the 2007 recommendations of the International Commission on Radiological Protection–the system of radiological protection in humans," *Ann. ICRP* **37**(2–4), 81–123 (2007).
8. M. Sidhu et al., "Image gently, step lightly: increasing radiation dose awareness in pediatric interventional radiology," *Pediatr. Radiol.* **39**(10), 1135–1138 (2009).
9. A. Roguin et al., "Brain and neck tumors among physicians performing interventional procedures," *Am. J. Cardiol.* **111**(9), 1368–1372 (2013).
10. E. Picano and E. Vano, "The radiation issue in cardiology: the time for action is now," *Cardiovasc. Ultrasound* **9**(1), 35 (2011).
11. S. Jacob et al., "Interventional cardiologists and risk of radiation-induced cataract: results of a French multicenter observational study," *Int. J. Cardiol.* **167**(5), 1843–1847 (2013).
12. N. J. Kleiman, "Radiation cataract," *Ann. ICRP* **41**(3–4), 80–97 (2012).
13. BCIS, *National Audit of Percutaneous Coronary Interventional Procedures Public Report: Annual Public Report Jaunuary 2012–December 2012*, UCL, London (2014).
14. R. G. Dixon and L. Wagner, "Managing image quality and patient dose in the angiography suite: do you really need that image quality?" *Tech. Vasc. Interventional Radiol.* **13**(3), 183–187 (2010).
15. J. Bushberg et al., Eds., *The Essential Physics of Medical Imaging*, 2nd ed., Wilkins, Philidelphia (2001).
16. A. Gislason-Lee et al., "Understanding automated dose control in dynamic x-ray imaging systems," in *European Congress on Radiology*, pp. 1–26, ECR, Vienna (2013). http://posterng.netkey.at/esr/viewing/index.php?module=viewing_poster&doi=10.1594/ecr2013/C-2183
17. W. J. H. Veldkamp et al., "A technique for simulating the effect of dose reduction on image quality in digital chest radiography," *J. Digital Imaging* **22**(2), 114–125 (2009).
18. R. S. Saunders and E. Samei, "A method for modifying the image quality parameters of digital radiographic images," *Med. Phys.* **30**(11), 3006 (2003).
19. BSI, *Medical Electrical Equipment—Characteristics of Digital X-Ray Imaging Devices—Part 1–3: Determination of the Detective Quantum Efficiency—Detectors Used in Dynamic Imaging*, London (2008).

20. P. A. Hiles and H. C. Starritt, *IPEM Report 32 (II) Measurement of the Performance Characteristics of Diagnostic X-Ray Systems Used in Medicine: X-Ray Image Intensifier Television Systems*, IPEM, York, UK (1996).
21. J. H. Launders et al., "Update on the recommended viewing protocol for FAXIL threshold contrast detail detectability test objects used in television fluoroscopy," *BJR* **68**(805), 70–77 (1995).
22. A. R. Cowen, "The physical evaluation of physical performance of TV fluoroscopy and digital fluorography systems using the Leeds x-ray test objects: a UK approach to QA in the diagnostic radiology department," in *American Association of Physicists in Medicine Monograph No. 20*, A. Seibert, G. T. Barnes, and R. G. Gould, Eds., pp. 499–568, AIP, Woodbury (1994).
23. P. A. Hiles et al., *IPEM Report 91 Recommended Standards for the Routine Performance Testing of Diagnostic X-Ray Imaging Systems*, IPEM, York, UK (2005).
24. F. A. A. Kingdom and N. Prins, *Psychophysics: A Practical Introduction*, Elsevier, London, UK (2010).
25. B. Treutwein, "Minireview: adaptive psychophysical procedures," *Vision Res.* **35**(17), 2503–2522 (1995).
26. H. Levitt, "Transformed up-down methods in psychoacoustics," *J. Acoust. Soc. Am.* 467–477 (1970).
27. M. A. García-Pérez, "Yes-no staircases with fixed step sizes: psychometric properties and optimal setup," *Optom. Vision Sci.* **78**(1), 56–64 (2001).
28. S. J. Shepard et al., *Quality Control in Diagnostic Radiology. Report of Task Group #12 Diagnostic X-Ray Imaging Committee*, Madison, Wisconsin (2002).
29. H. Lai and A. Cunningham, "Noise aliasing in interline-video-based fluoroscopy systems," *Med. Phys.* **29**(3), 298–310 (2002).
30. D. P. Frush et al., "Computer-simulated radiation dose reduction for abdominal multidetector CT of pediatric patients," *Am. J. Roentgenol.* **179**, 1107–1113 (2002).
31. A. J. Britten et al. "The addition of computer simulated noise to investigate radiation dose and image quality in images with spatial correlation of statistical noise: an example application to x-ray CT of the brain," *Br. J. Radiol.* **77**(916), 323–328 (2004).
32. M. Söderberg, M. Gunnarsson, and M. Nilsson, "Simulated dose reduction by adding artificial noise to measured raw data: a validation study," *Radiat. Prot. Dosim.* **139**(1–3), 71–77 (2010).
33. C. Won Kim and J. H. Kim, "Realistic simulation of reduced-dose CT with noise modeling and sinogram synthesis using DICOM CT images," *Med. Phys.* **41**(1), 011901 (2014).
34. P. Massoumzadeh et al., "Validation of CT dose-reduction simulation," *Med. Phys.* **36**(1), 174–189 (2009).
35. R. Tanaka et al., "Review of a simple noise simulation technique in digital radiography," *Radiology* **5**, 178–185 (2012).
36. M Båth et al., "Method of simulating dose reduction for digital radiographic systems," *Radiat. Prot. Dosim.* **114**(1–3), 253–259 (2005).
37. O. Treiber et al., "An adaptive algorithm for the detection of microcalcifications in simulated low-dose mammography," *Phys. Med. Biol.* **48**(4), 449–466 (2003).
38. A. Svalkvist and M. Båth, "Simulation of dose reduction in tomosynthesis," *Med. Phys.* **37**(1), 258 (2010).
39. P. Rauch et al., *Functionality and Operation of Fluoroscopic Automatic Brightness Control/Automatic Dose Rate Control Logic in Modern Cardiovascular and Interventional Angiography Systems: A Report of Task Group 125 Radiography/Fluoroscopy Subcommittee, Imaging Physics Co.*, Vol. **39** (2012).
40. M. J. Tapiovaara, M. Sandborg, and D. R. Dance, "A search for improved technique factors in paediatric fluoroscopy," *Phys. Med. Biol.* **44**, 537–559 (1999).
41. A. J. Gislason, A. G. Davies, and A. R. Cowen, "Dose optimization in pediatric cardiac x-ray imaging," *Med. Phys.* **37**(10), 5258–5269 (2010).
42. A. J. Gislason-Lee et al., "Dose optimization in cardiac x-ray imaging," *Med. Phys.* **40**, 091911 (2013).
43. D. L. Wilson, P. Xue, and R. Aufrichtig, "Perception of fluoroscopy last-image hold," *Med. Phys.* **21**(12), 1875–1883 (1994).
44. R. Aufrichtig et al., "Perceptual comparison of pulsed and continuous fluoroscopy," *Med. Phys.* **21**(2), 245–256 (1994).
45. K. N. Jabri and D. L. Wilson, "Quantitative assessment of image quality enhancement due to unsharp-mask processing in x-ray fluoroscopy," *J. Opt. Soc. Am. A Opt. Image Sci. Vision* **19**(7), 1297–1307 (2002).
46. K. N. Jabri and D. L. Wilson, "Detection improvement in spatially filtered x-ray fluoroscopy image sequences," *America (NY)* **16**(3), 742–749 (1999).
47. D. L. Wilson et al., "Perceived noise versus display noise in temporally filtered image sequences," *J. Electron. Imaging* **5**(4), 490–495 (1996).
48. P. Xue et al., "An adaptive reference/test paradigm: application to pulsed fluoroscopy perception," *Behav. Res. Methods Instrum. Comput* **30**(2), 332–348 (1998).
49. Y. Srinivas and D. L. Wilson, "Image quality evaluation of flat panel and image intensifier digital magnification in x-ray fluoroscopy," *Med. Phys.* **29**(7), 1611–1621 (2002).
50. M. Båth, "Evaluating imaging systems: practical applications," *Radiat. Prot. Dosim.* **139**(1–3), 26–36 (2010).
51. M. J. Tapiovaara, "Review of relationships between physical measurements and user evaluation of image quality," *Radiat. Prot. Dosim.* **129**(1–3), 244–248 (2008).
52. A. Tingberg et al., "What is worse: decreased resolution or increased noise?" *Proc. SPIE* **4686**, 338–346 (2002).
53. S. M. Kengyelics et al., "Context sensitive cardiac x-ray imaging: a machine vision approach to x-ray dose control," *J. Electron. Imaging*, **24**(5), 051002 (2015).
54. M. G. Andreassi et al., "Cardiac catheterization and long-term chromosomal damage in children with congenital heart disease," *Eur. Heart J.* **27**(22), 2703–2708 (2006).

Amber J. Gislason-Lee is a medical physicist based at the University of Leeds, UK. She received her BSc degree from the University of Winnipeg, Canada, and her MSc in medical physics from University of Leeds. Her research has included pediatric dose optimization in diagnostic radiology and quantifying performance of cardiac flat-panel detector based interventional x-ray imaging systems.

Asli Kumcu is a PhD candidate at Ghent University. She received her BS degree in electrical engineering from Purdue University in 2002, her MS degree in medical imaging from University of Leuven in 2008, and worked for a number of years in the medical imaging industry. Her research interests include image and video quality evaluation and optimization of medical imaging devices.

Stephen M. Kengyelics received his MSc degree in physics from the University of Leeds, United Kingdom, in 1997. He received his BEng degree in electrical and electronic engineering from the University of Plymouth in 1991. His research has included quantifying the performance of medical x-ray image detectors and the application of machine vision to interventional cardiac x-ray imaging.

David S. Brettle is the head of medical physics and engineering in the Leeds Teaching Hospitals. His main areas of work have been in diagnostic radiology—including radiation protection, medical imaging, and psychophysics. He is an accredited radiation protection advisor and medical physics expert in diagnostic radiology. He has over 50 publications and a portfolio of innovation activity. He is also an honorary professor of health science at the University of Salford.

Laura A. Treadgold is a lecturer in medical imaging and the associate director of student education in the School of Medicine at the University of Leeds, United Kingdom. She received her PhD in chemistry in 2002, her BSc degree in applied chemistry with biochemistry medicine in 1997, and her research interests are in dual x-ray absorptiometry.

Mohan Sivananthan is a professor of cardiac imaging intervention and a consultant in cardiac interventions. As both as a radiologist and cardiologist, he has a keen interest in radiation dose optimization. He has been performing interventional procedures for 25 years, during which time he has been actively involved in innovative cardiac imaging research.

Andrew G. Davies is a lecturer in medical imaging at the University of Leeds, United Kingdom, where he received his MSc degree in medicine in 1995 and his BSc degree in computer science in 1990. His research interests include image quality, system performance, and optimization of medical x-ray imaging systems.